NASA TECHNICAL NOTE

NASA TN D-6384

EXPERIMENTAL INVESTIGATION OF SELF-ACTING-LIFT-PAD CHARACTERISTICS FOR MAIN-SHAFT SEAL APPLICATIONS

by William F. Hady and Lawrence P. Ludwig

Lewis Research Center
Cleveland, Ohio 44135

NATIONAL AERONAUTICS AND SPACE ADMINISTRATION • WASHINGTON, D. C. • OCTOBER 1971

1. Report No.	2. Government Accession No.	3. Recipient's Catalog No.
NASA TN D-6384		

4. Title and Subtitle
EXPERIMENTAL INVESTIGATION OF SELF-ACTING-LIFT-PAD CHARACTERISTICS FOR MAIN-SHAFT SEAL APPLICATIONS

5. Report Date
October 1971

6. Performing Organization Code

7. Author(s)
William F. Hady and Lawrence P. Ludwig

8. Performing Organization Report No.
E-6186

10. Work Unit No.
126-15

9. Performing Organization Name and Address
Lewis Research Center
National Aeronautics and Space Administration
Cleveland, Ohio 44135

11. Contract or Grant No.

13. Type of Report and Period Covered
Technical Note

12. Sponsoring Agency Name and Address
National Aeronautics and Space Administration
Washington, D.C. 20546

14. Sponsoring Agency Code

15. Supplementary Notes

16. Abstract
Experimental studies on four self-acting-lift geometries (shrouded step pads) for maintaining positive separation of seal surfaces are compared with theoretical calculations. Load capacities at measured film thicknesses were lower than those predicted by theory for parallel surfaces. Sufficient gas (air) film stiffness was generated so that dynamic tracking of the seal seat face runout was maintained. Seal seat runouts to 0.0089 cm (0.0035 in.) were accommodated. Tracking, however, is inhibited during startup under light loads when seal seat runouts exceed 0.0025 cm (0.001 in.).

17. Key Words (Suggested by Author(s))
Self-acting seal
Hydrodynamic lift
Shrouded step pad

18. Distribution Statement
Unclassified - unlimited

19. Security Classif. (of this report)	20. Security Classif. (of this page)	21. No. of Pages	22. Price*
Unclassified	Unclassified	21	$3.00

*For sale by the National Technical Information Service, Springfield, Virginia 22151

EXPERIMENTAL INVESTIGATION OF SELF-ACTING-LIFT-PAD CHARACTERISTICS FOR MAIN-SHAFT SEAL APPLICATIONS

by William F. Hady and Lawrence P. Ludwig

Lewis Research Center

SUMMARY

Experimental studies were made to determine load capacities, measure gas film thicknesses, and gain more insight into the operation of self-acting-lift geometries (shrouded step pads) for maintaining positive separation of sealing surfaces. Four geometries, all having a 12.00-centimeter (4.75-in.) mean diameter and a radial width of 0.51 centimeter (0.20 in.) were run at a rotative speed of 61 meters per second (200 ft/sec), an ambient pressure of 10 newtons per square centimeter (14.7 lb/in.^{2}), and room temperature, 300 K (80° F).

Measurements of the gas film thickness indicated that the seal ring closely followed the face runout of the rotating seal seat with no detectable phase shift in the relative movements. The amplitude of the seal ring response to seal seat runout is a function of the amount of runout as well as the seal spring load. The results show that seal seat runout should be limited to 0.0025 centimeter (0.001 in.) or less as tracking is inhibited during startup under light loads. Measurements of the maximum load capacities are lower than theoretical calculations predict for parallel surfaces. A maximum load of 12.5 kilograms (27.5 lb) was obtained with a recess-pad-length to land-length ratio of 2:1 and a recess-pad depth of 0.0013 centimeter (0.0005 in.). The calculated film stiffness for the best geometry (operating at a film thickness of 0.00025 cm (0.0001 in.)) was 0.5×10^5 kilograms per centimeter (3×10^5 lb/in.). The compressibility numbers for this investigation ranged from 4 to 80, values approximately four times greater than those projected for advanced aircraft applications.

INTRODUCTION

Advanced airbreathing engines will require the development of main-shaft seals that can withstand severe environmental conditions. Seals will be required to operate

at surface speeds of 152 meters per second (500 ft/sec) (ref. 1), pressure differentials of 345 newtons per square centimeter (500 lb/in.^{2}), and temperatures in excess of 977 K (1300° F) (ref. 2). At present, conventional face seals are limited to surface speeds of 107 meters per second (350 ft/sec), pressure differentials to 86.1 newtons per square centimeter (125 lb/in.^{2}), and gas temperatures to 700 K (800° F) (ref. 3). Because of the increased severity of the environmental conditions, it is imperative that face seals operate with a positive face separation in order to obtain long life and reliability. The most direct approach to the problem of obtaining positive face separation is through the use of hydrostatic (either system or external pressure actuated) or self-acting lift geometries incorporated in face seal designs, as reported in references 3 to 5.

Recent seal testing of a self-acting design (ref. 6) at a speed of 122 meters per second (400 ft/sec), a pressure of 172 newtons per square centimeter (250 lb/in.^{2}), and a sealed gas temperature of 810 K (1000° F) has indicated satisfactory performance. These tests demonstrate that the self-acting seals operate without rubbing contact and apparently operate at or near the design clearance (calculated by means of a mathematical model from measured leakage data). Actual measurements of this operating clearance (gas film thickness) are desirable, however, because the mathematical model at present does not consider the effect of axial movement (such as face runout) on this gas film thickness or the response of the seal ring to these axial movements. It is thought that face runout will result in rapid changes of the instantaneous film thickness and cause it to vary circumferentially around the seal. This variation is therefore a concern: a maximum instantaneous film thickness from a leakage standpoint and a minimum instantaneous film thickness from a rubbing or wear standpoint.

In addition to maintaining positive face separation, the self-acting lift geometries provide a means of obtaining the proper force balance within the seal system. This force balance, directly related to the load carrying capacity (generated lift force) of the self-acting geometry, must be accurately known in order to obtain the designed gas film thickness. Mathematical models provide a method for determining the load carrying capacity; however, actual measurements are desired because the mathematical model also indicates a reduction in load carrying capacity when the sealing faces are not parallel. In practical seal applications, where thermal gradients and pressure distortions are present, the probability of maintaining force parallelism is very slight.

The objectives of this investigation of self-acting lift geometries were to (1) measure load capacities, (2) measure seal lift (gas film thickness), (3) calculate the gas film stiffness, and (4) compare experimental data with theoretical calculations as set forth in reference 7 and understand those factors more fully as they relate to the operation or dynamic tracking of a face seal having self-acting lift augmentation.

In this investigation, the sealing dam of the face seal has been omitted in order to study the self-acting lift pad separately. Because of inherent instrumentation problems

associated with elevated temperatures, these studies were made at room temperature, 300 K (80° F), ambient pressure P_1, 10 newtons per square centimeter (14.7 lb/in.^{2}), and a rotative speed of 61 meters per second (200 ft/sec). Four geometries, all having a 12.00-centimeter (4.75-in.) mean diameter and 15 shrouded step pads, were located on the rotating seat.

APPARATUS

The seal test apparatus used in these studies, shown schematically in figure 1, consists of two separate housings. The fixed bearing support housing contains the shaft support bearings and associated oil and air lines. An overhanging shaft, approximately 15.24 centimeters (6.00 in.) long, can accommodate rotating seal seats to a nominal 25.40-centimeter (10.00-in.) diameter. Maximum rotative speed, 10 000 rpm, is controlled by a variable-speed dc motor coupled through a 1:4 speed increaser.

The movable seal ring housing, which can move axially by means of four lead screws coupled together by sprockets and a continuous chain, contains the stationary seal ring. The load is applied to the seal ring through 16 compression springs (rated at 5.73 kg/cm (32 lb/in.)) and can be varied from 0 to 165 kilograms (75 lb) during testing. The housing itself is mounted on a precision slide (not shown) that allows the housing to be moved back for ease of access to the seal seat and the seal ring during setup.

Self-Acting-Lift-Pad Geometries

Face seals with self-acting lift pads that are in use or in the testing phase to date generally have the lift pads and the sealing dam machined into the nonrotating seal ring. In this investigation, however (see fig. 2), the geometries were machined (electrical discharge machined) into the rotating seal seat. The seal seat was made of AISI 4340 carbon steel, ground and lapped parallel to within 0.00051 centimeter (0.0002 in.) and flat within two helium light bands. Also in this investigation, the sealing dam (cross-hatched area of seal ring) was removed to allow for independent study of the self-acting geometries. Because the geometries were machined into the seal seat, the shrouds (shown by imaginary lines in section A-A) were formed by machining the carbon seal ring face selectively so that it extended beyond the radial width of the lift pad by the required 0.051 centimeter (0.020 in.) of this study. The carbon seal ring (designated a high-temperature carbon) was also lapped to within two helium light bands of flatness. It should be noted that the lift-pad geometries are bounded by an ambient pressure P_1. In practice this is accomplished by radial feed grooves that connect the sealed pressure with an annular groove located inside the sealing dam.

Selection of the lift-pad geometries was based primarily on the optimum geometry described in reference 7. Figure 3 shows the actual dimensions of the self-acting-lift-pad geometries used in this investigation. Fifteen pads were equally spaced on a 12.00-centimeter (4.75-in.) mean diameter. Figure 4 shows the seal seat having a 2:1 recess-pad-length to land-length ratio.

Instrumentation

The instrumentation system used to detect and record the lift movement of the seal ring and the seal seat face runout used miniature capacitance probes as the primary gap-height sensors. The probes, designed and fabricated at NASA Lewis, are designated 5-mil probes; they were 0.76 centimeter (0.30 in.) long and had a nominal 0.47-centimeter (0.19-in.) diameter and an approximate weight of 10 grams (0.02 lb). Movement as small as 0.000025 centimeter (0.00001 in.) can be discerned with a read-out accuracy of approximately ±3 percent. The output of the sensors, monitored by a distance meter, was fed into a dc amplifier, which in turn was fed into a 24-channel oscillograph. The instrumentation was also capable of monitoring, during testing, the sensor output on a 4-channel oscilloscope. In addition, a 14-channel tape recorder was available for storage of data for future playback.

Figure 5 shows schematically the relative positions of two capacitance probes used in this investigation. In order to obtain continuous face runout measurements it was necessary to locate probe 5 as shown (45° from the vertical). Justifying this placement requires that the seal seat face parallelism be held to 0.00051 centimeter (0.0002 in.). Therefore, prior to actual testing, another probe was located so that runout of both faces could be directly compared at maximum rotative speed. If the seal seat parallelism is within the specified limits, it is possible to use the back face as an indication of seal seat runout, as the front face runout will be a mirror image.

Figure 6 shows the seal ring with the four capacitance probes in position. The four probes mounted in the seal ring carrier detected the amount of separation (or lift) of the two sealing surfaces as well as the movement of the seal ring relative to the seal seat runout. To allow for possible seal closing or rubbing, these probes were located approximately 0.0051 centimeter (0.002 in.) below the height of the carbon. The probes were located at 45°, 135°, 225°, and 270° from the vertical. Probe 1, at 45°, was therefore directly opposite the seal seat face runout probe 5.

Also shown in figure 6 is the placement of one thermocouple centrally located between the inside and outside diameter of the carbon face and approximately 0.076 centimeter (0.030 in.) beneath the surface. This thermocouple was used to detect a temperature rise in the carbon due to frictional heating when the carbon seal ring came in contact with the rotating seal seat.

RESULTS AND DISCUSSION

Theory and Experimental Data

Dynamic seal studies were made to provide the needed experimental background in using self-acting-lift geometries for maintaining positive separation of sealing surfaces. All of the tests were conducted at a rotative speed of 61 meters per second (200 ft/sec), ambient pressure of 10 newtons per square centimeter (14.7 lb/in.^{2}), and room temperature, 300 K (80° F). Self-acting-lift geometry data are presented to show the response of the seal ring to face runout of the seal seat as well as the effect of spring load on this response. The measured load capacities and gas film thickness measurements are compared with theoretical calculations obtained from a modified form of the computer program of reference 7. The computer program of reference 7 was modified to allow numerical solutions for high compressibility numbers.

Figures 7 to 10 are used to show how the seal ring responds to the face runout of the seal seat as the amount of face runout is varied and to show the effect of spring load on this response. Figures 7 and 8 show the effect of spring load on the seal ring response to a 0.0021-centimeter (0.00085-in.) runout of the seal seat. The oscillograph traces of figure 7 indicate that the seal ring response (as measured by probes 1 and 3) is a periodic variation that is in phase with the seal seat runout (as measured by probe 5 located opposite probe 1, see fig. 5) and is most apparent at the lower spring load of 4.53 kilograms (10 lb). This in-phase relation is of interest because it pinpoints the mode of vibration to be expected for this type of seal and should be helpful in formulating future theoretical studies on seal vibration response.

Another significant point to be noted in figure 7 and shown further in figure 8 is that the magnitude of the variation of the seal ring response decreases with increasing spring load. This variation in seal ring response, which is a change in the gas film thickness, indicates that instantaneous maximum and minimum film thicknesses are a result of seal seat runout. These changes in gas film thickness would be of concern in actual seal applications from a leakage standpoint (maximum film thickness) as well as from a rubbing or wearing standpoint (minimum film thickness). The arithmetical average film thickness is also of importance from a theoretical standpoint because it is the basis for calculating the film stiffness as well as an experimental check on theory.

The oscillograph traces of figure 9 show the effect of seal seat runout on seal ring response under a light spring load of 1.13 kilograms (2.50 lb). (Note that the scale for the seal ring runout of 0.00051 cm (0.0002 in.) is twice that for the seal seat runout.) The important point is that, as the seal seat runout increases from 0.00051 to 0.0022 centimeter (0.0002 to 0.00085 in.), the magnitude of the seal ring response also increases (nearly as much as the seal seat runout in both cases) and is also in phase, as

noted previously for figure 7. For these lightly loaded conditions it appears that the inertia forces resulting from the seal seat runout are sufficient to cause unstable operation. Although the average film thickness for the 0.0022-centimeter (0.00085-in.) runout is of the order of 0.0008 centimeter (0.00033 in.), the measured minimum film thickness (in addition to a temperature rise in the carbon of the seal ring) indicated that the seal ring was intermittently touching down. Visual inspection of the seal ring after 5 minutes of unstable operation showed the carbon ring to be rubbing at the inside diameter. This would indicate that there is a slight coning of either the seal seat or the carbon mounted in the seal ring.

Figure 10 shows oscilloscope traces illustrating the ability of the shrouded lift-pad geometry to compensate for seal seat runout excursions, while maintaining dynamic tracking, even though the face runouts ranged from 0.0022 to 0.0089 centimeter (0.00085 to 0.0035 in.). From these photographs it is concluded that sufficient gas film stiffness and viscous fluid damping (which are dependent on low compressibility numbers) were provided by the self-acting geometry. Compressibility, which is defined as $\Lambda = 6\mu U/ph^2$, where μ is fluid viscosity, U is seal velocity, p is ambient pressure, and h is fluid film thickness, is very dependent on pressure; the higher the pressure, the lower the compressibility number. Better dynamic tracking is therefore the result of lower compressibility. In this investigation, however, the compressibility numbers ranged from 4 at a gap height of 0.001 centimeter (0.0004 in.) to 80 at a gap height of 0.00025 centimeter (0.0001 in.). These numbers are approximately four times greater than those shown in Table II of reference 7. Testing at atmospheric pressures, which results in high compressibility numbers, should therefore impose a more severe test than will be required for future main-shaft seal applications because of the low gas film stiffness and viscous fluid damping at this pressure. The lower rotative speeds of this investigation, however, may not be representative of the excitation frequency that could be expected in future applications and should be increased in future studies.

From figures 7 to 10 three significant facts can be noted that permitted the seal ring to track the seal seat face runout dynamically at the conditions of this investigation:

(1) Face runout of the seal seat should be held to 0.00051 centimeter (0.0002 in.) in order to minimize seal ring movement under lightly loaded conditions.

(2) Face runouts of the order of 0.0025 centimeter (0.001 in.) should be avoided. However, if sufficient spring load is provided, the seal ring movement can be minimized and satisfactory operation of the seal can be expected.

(3) With sufficient load, seal seat runout excursions of the order of 0.0089 centimeter (0.0035 in.) were accommodated and dynamic tracking of the seal seat was maintained.

Figures 11 and 12 are comparisons of the test results with theoretical calculations showing the load capacity (generated lift force) of the four self-acting lift geometries as

a function of film thickness. In all cases, the load capacity increases as the film thickness decreases. The most effective geometry had a 2:1 recess-pad-length to land-length ratio and a recess-pad depth of 0.0013 centimeter (0.0005 in.), the maximum load being 12.5 kilograms (27.5 lb). The calculated film stiffness (which can be interpreted as a change in film thickness due to a change in applied load from its steady-state equilibrium conditions, ref. 7) is of the order of 0.5×10^5 kilogram per centimeter (3×10^5 lb/in.) when the seal is operating at a film thickness of 0.00025 centimeter (0.0001 in.).

Three other significant facts can be observed in figures 11 and 12 relative to the test conditions of this investigation:

(1) The self-acting-lift geometries having a 2:1 recess-pad-length to land-length ratio were more effective in generating lift and providing a higher gas film stiffness than those having the 1:1 ratio.

(2) The shallower recess-pad depth of 0.0013 centimeter (0.0005 in.) was also more effective than the 0.0025-centimeter (0.001-in.) depth in generating lift (supporting more load).

(3) There is a significant difference in the measured load capacities as compared with calculated load capacities where parallel surfaces are assumed. This difference may have been caused by operating the seal with slightly nonparallel surfaces, either converging or diverging in nature.

A seal with exaggerated face distortion or tilt is illustrated in figure 13. Theoretical calculations of load capacity where a condition of nonparallelism is assumed (ref. 7) show a reduction in load capacity for a given lift-pad geometry and set of operating conditions. In this investigation, if an angular tilt of 0.0025 centimeter (0.0001 in.) is assumed, the measured load capacities do closely agree with theoretical calculations. No attempt was made during this investigation to measure angular tilt; however, wear patterns obtained while operating the seal at or near rubbing contact suggest that the seal was operating with a slight diverging tilt. Surface profile traces of the carbon seal ring after testing were inconclusive as to the degree of tilt because rubbing occurred only at the inside diameter. The effect of this tilt on load capacity was that of reducing the load capacity from a calculated load of 22.4 kilograms (49.3 lb) (parallel surfaces assumed) to a measured load of 12.5 kilograms (27.5 lb) for the most effective geometry of this investigation.

It should be mentioned that distortion can be the result of one or a combination of several of the following inherent conditions associated with dynamic seal applications. Each of these conditions takes on increased importance because of the more severe environmental conditions imposed on the seal and should be avoided or at least held to a minimum.

(1) Distortion due to thermal gradients (see ref. 3)

(2) Distortion due to centripetal forces of the rotating seat resulting from an unsymmetrical design

(3) Distortion due to improper design of seal components resulting from high pressure loading

(4) Distortion resulting from tolerance buildup during fabrication as well as improper installation of seal components

Visual Observations

Several visual observations pertinent to the evaluation of self-acting-lift geometries for seal applications, and not readily apparent from the data presented, indicate the following:

(1) During startups and shutdowns, lift-off or separation of the seal faces occurs and is maintained at relatively low rotating velocities. Under maximum load conditions, each geometry indicated seal ring lift at speeds in the range of 6.1 meters per second (20 ft/sec) to 18.3 meters per second (60 ft/sec).

(2) During startup under light load conditions, a seal seat face runout of 0.0025 centimeter (0.001 in.), and an acceleration of 0 to 61 meters per second (0 to 200 ft/sec) in 10 seconds, the forces exerted by the seal seat were too large for the spring load to overcome. Attempts to dampen out or decrease seal ring movement by applying more load when the maximum rotative speed was reached resulted in excessive rubbing and high seal temperatures (600 K; 648° F).

(3) Operating a seal with self-acting-lift geometries at or near its maximum hydrodynamic load capacity is not a desirable situation. In this investigation, a further increase in the applied axial load (approximately 0.29 kg; 0.63 lb) resulted in excessive rubbing of the mating surfaces. When this occurred, seal temperatures in excess of 600 K (648° F) were recorded.

SUMMARY OF RESULTS

An experimental study was made to gain an insight into the capabilities and limitations of a face seal with self-acting-lift geometries used for maintaining positive surface separation. The four geometries consisted of recess-pad-length to land-length ratios of 2:1 and 1:1 and recess-pad depths of 0.0025 and 0.0013 centimeter (0.001 and 0.0005 in.). The self-acting geometry was located on the seal seat having a 12.00-centimeter (4.75-in.) mean diameter. Operating test conditions were rotative speed, 61 meters per second (200 ft/sec); atmospheric pressure, 10 newtons per square centimeter (14.7 lb/in.^{2}); and room temperature of 300 K (80° F).

The results of this study were compared with theoretical calculations, and the following results were noted:

1. All of the self-acting geometries, within the range of loads and at the ambient pressure of this investigation, provided sufficient film stiffness, allowing the seal ring to track the seal seat runout dynamically.

a. The highest film stiffness, of the order of 0.5×10^5 kilograms per centimeter (3×10^5 lb/in.), was obtained with a recess-pad-length to land-length ratio of 2:1 and a recess-pad depth of 0.0013 centimeter (0.0005 in.) operating at an average film thickness of 0.00025 centimeter (0.0001 in.).

b. Face runouts ranging from 0.0013 to 0.0025 centimeter (0.0005 to 0.001 in.) were easily accommodated. Film thickness measurements indicated the seal was operating at an average thickness of 0.00025 centimeter (0.0001 in.) down to a minimum film thickness of 0.00013 centimeter (0.00005 in.) under maximum load conditions.

c. Shaft instabilities that resulted in excessive seal seat face runouts, ranging to a high of 0.0089 centimeter (0.0035 in.), were also accommodated; however, sufficient axial load was required to overcome the forces exerted by the seal seat.

d. Compressibility numbers that were calculated for the conditions of this investigation ranged from 4 to 80 and are approximately four times greater than those predicted for advanced aircraft turbine engine main-shaft seal applications.

2. All the measured load capacities of the four lift-pad geometries in this investigation were lower than theoretical calculations predict for parallel surfaces.

a. A maximum load capacity of 12.5 kilograms (27.50 lb) was obtained with the recess-pad-length to land-length ratio of 2:1, and a recess depth of 0.0013 centimeter (0.0005 in.) operating at a film thickness of 0.00025 centimeter (0.0001 in.).

b. Increasing the axial load by 0.29 kilogram (0.63 lb) when operating the seal at or near its maximum hydrodynamic load capacity resulted in loss of surface separation. Peak temperatures in excess of 600 K (648° F) were measured within the carbon seal ring. Reducing the load again allowed the seal to lift off, if the seal was not permitted to rub for too long (longer than 2 min).

3. In these studies there appears to be a minimum load that must be applied to ensure stable operation during startup that is a function of seal seat runout and the apparent 0.00025-centimeter (0.0001-in.) tilt radially across the pad.

Lewis Research Center,
National Aeronautics and Space Administration,
Cleveland, Ohio, March 8, 1971,
126-15.

REFERENCES

1. Schevchenko, Richard P.: Shaft, Bearing and Seal Systems for a Small Engine. Paper 670064, SAE, Jan. 1967.

2. McKibbin, A. H.; and Parks, A. J.: Aircraft Gas Turbine Mainshaft Face Seals - Problems and Promises. Paper FICFS-28, ASLE, May 1969.

3. Parks, A. J.; McKibbin, A. H.; and Ng, C. C. W.: Development of Main Shaft Seals for Advanced Air Breathing Propulsion Systems. Rep. PWA-3161, Pratt & Whitney Aircraft (NASA CR-72338), Aug. 14, 1967.

4. Hawkins, R. M.: Development of Compressor End Seals, Stator Interstage Seals, and Stator Pivot Seals in Advanced Air Breathing Propulsion Systems. Rep. PWA-2875, Pratt & Whitney Aircraft (NASA CR-83786), July 20, 1966.

5. Hawkins, R. M.; McKibbin, A. H.; and Ng, C. C. W.: Development of Compressor Seals, Stator Interstage Seals, and Stator Pivot Seals in Advanced Air Breathing Propulsion Systems. Rep. PWA-3147, Pratt & Whitney Aircraft (NASA CR-95946), July 20, 1967.

6. Povinelli, V. P.; and McKibbin, A. H.: Development of Mainshaft Seals for Advanced Air Breathing Propulsion Systems - Phase II. Rep. PWA-3933, Pratt & Whitney Aircraft (NASA CR-72737), June 23, 1970.

7. Zuk, John; Ludwig, Laurence P.; and Johnson, Robert L.: Design Study of Shaft Face Seal With Self-Acting Lift Augmentation. I - Self-Acting Pad Geometry. NASA TN D-5744, 1970.

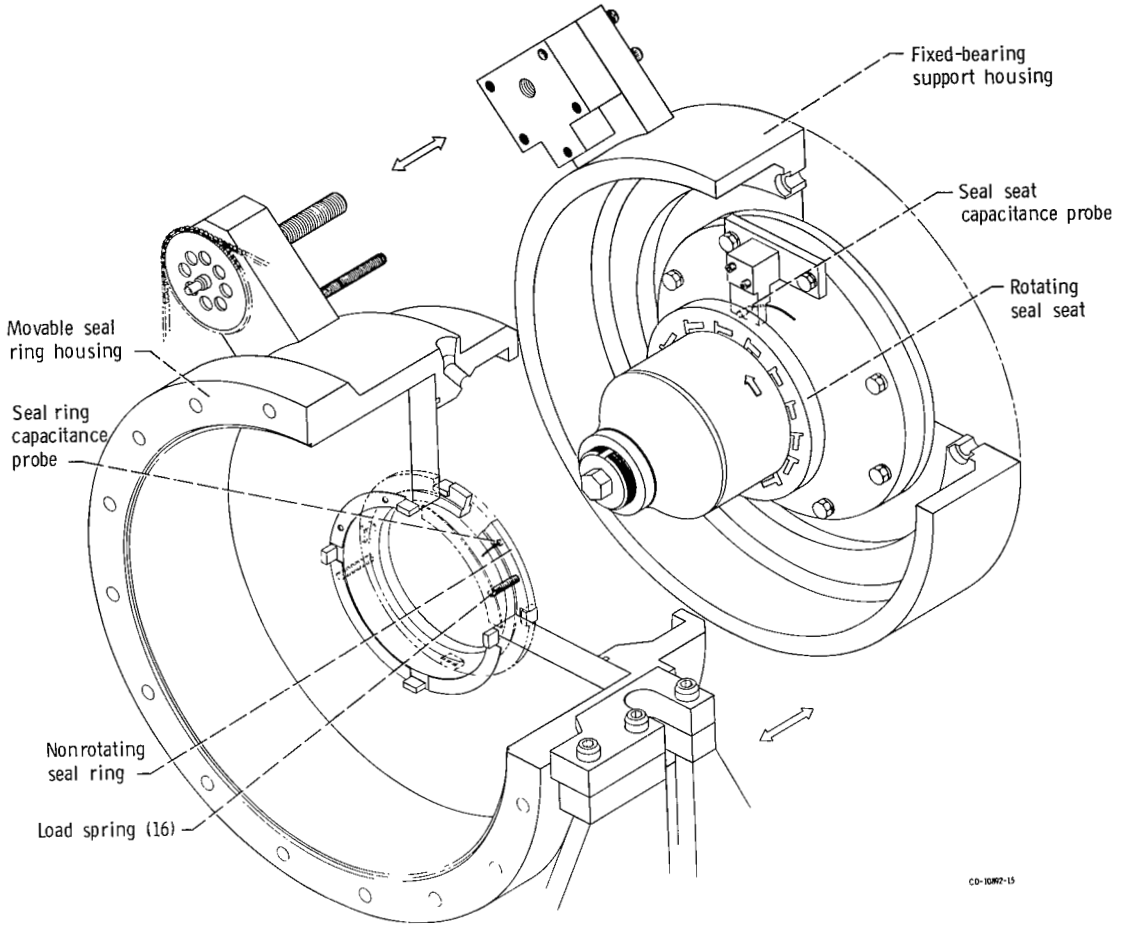

Figure 1. - High-speed seal test apparatus.

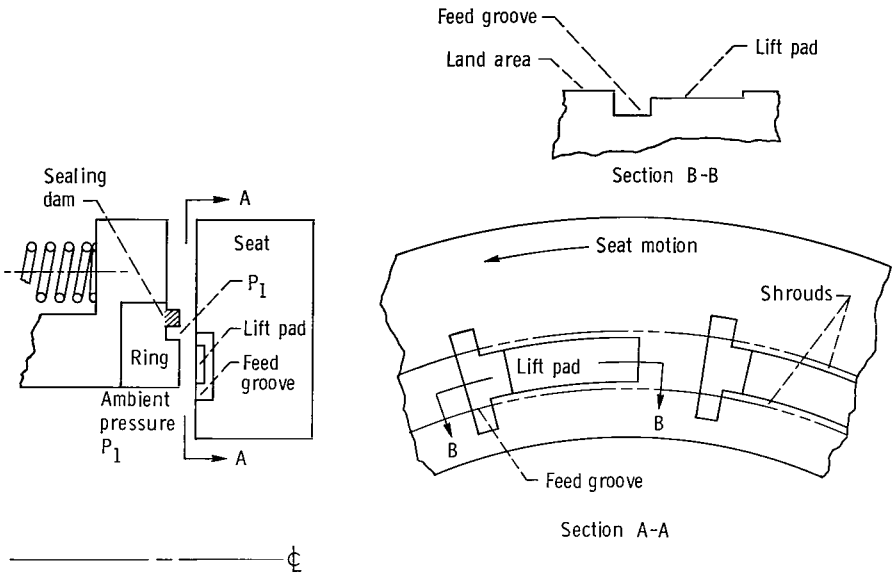

Figure 2. - Face seal with self-acting lift pads in rotating seat.

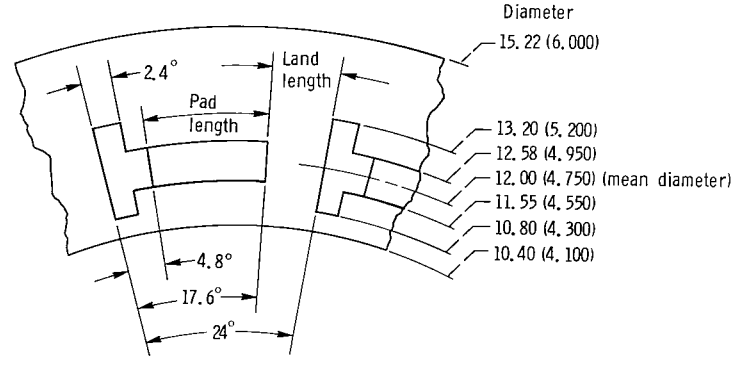

(a) 2:1 Ratio.

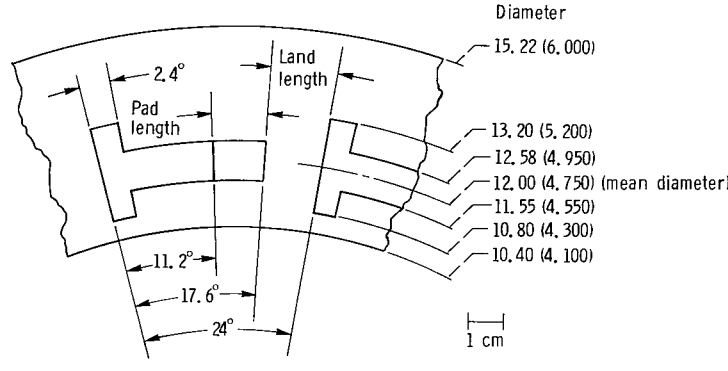

(b) 1:1 Ratio.

Figure 3. - Details of self-acting-lift-pad geometries used in this investigation. Feed groove depth, 0.08 centimeter (0.03 in.); pad depth, 0.0025 and 0.0013 centimeter (0.001 and 0.0005 in.). (All dimensions are in centimeters (in.).)

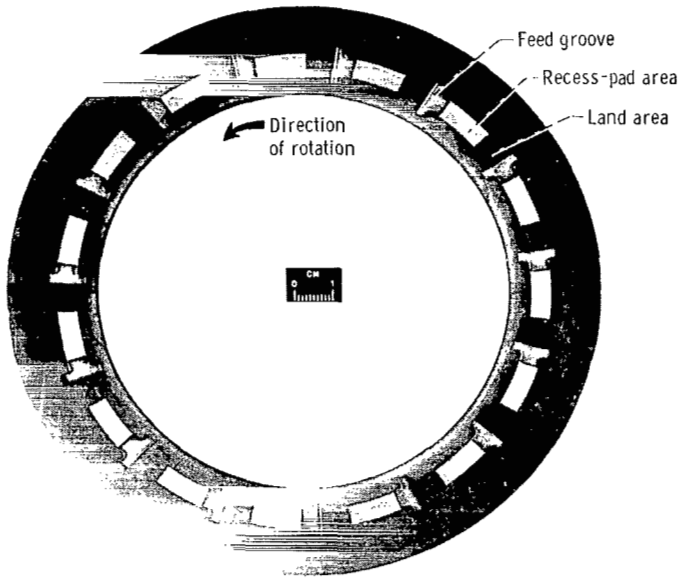

C-70-3027

Figure 4. - Rotating seal seat with recess-pad-length to land-length ratio of 2:1. Recess-pad depth, 0.0013 centimeter (0.0005 in.); radial feed groove depth, 0.076 centimeter (0.030 in.).

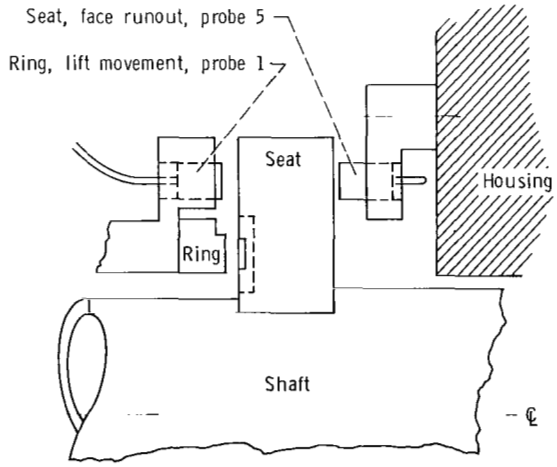

Figure 5. - Capacitance probe relative positions used in self-acting-lift-pad studies.

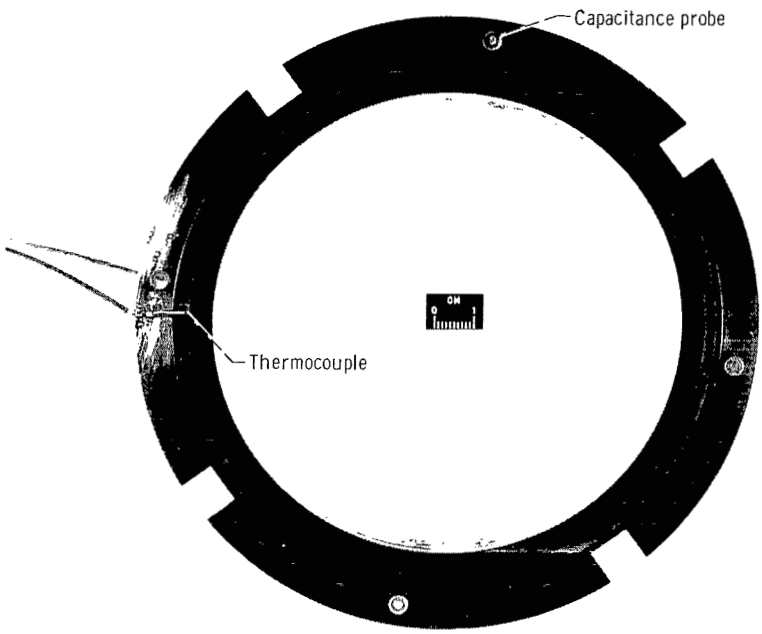

C-70-3026

Figure 6. - Capacitance probe and thermocouple pacement in seal ring carrier used in self-acting-lift-pad studies.

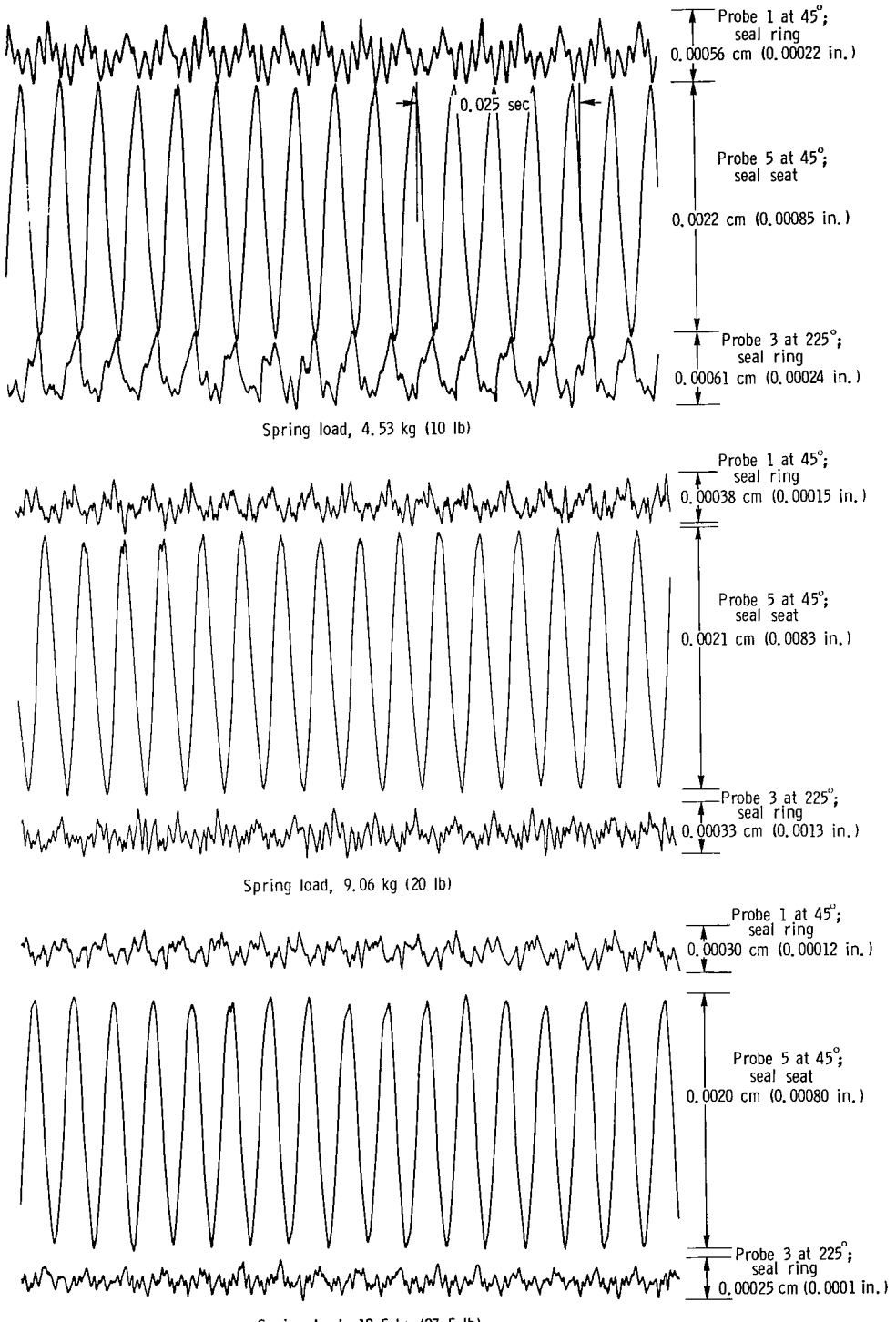

Figure 7. - Oscillograph traces showing effect of spring load on seal ring movement (relative to seal seat face). Average seal seat face runout, 0.0021 centimeter (0.00083 in.) recess-pad-length to land-length ratio, 2:1; recess-pad depth, 0.0013 centimeter (0.0005 in.); sliding velocity, 61 meters per second (200 ft/sec); ambient pressure, 10 newtons per square centimeter (14.7 lb/in.^{2}); room temperature, 300 K (80° F).

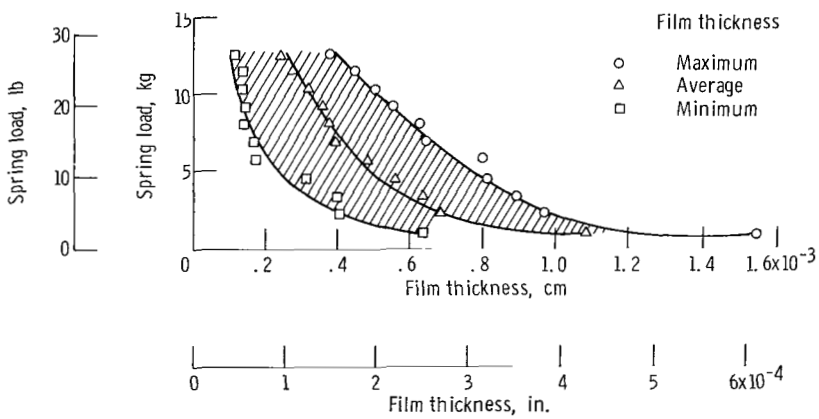

Figure 8. - Seal ring response as function of spring load showing measured maximum and minimum film thicknesses. Average seal seat face runout, 0.0021 centimeter (0.00083 in.); recess-pad-length to land-length ratio, 2:1; recess-pad depth, 0.0013 centimeter (0.0005 in.); sliding velocity, 61 meters per second (200 ft/sec); ambient pressure, 10 newtons per square centimeter (14.7 lb/in.^{2}); room temperature, 300 K (80^0 F).

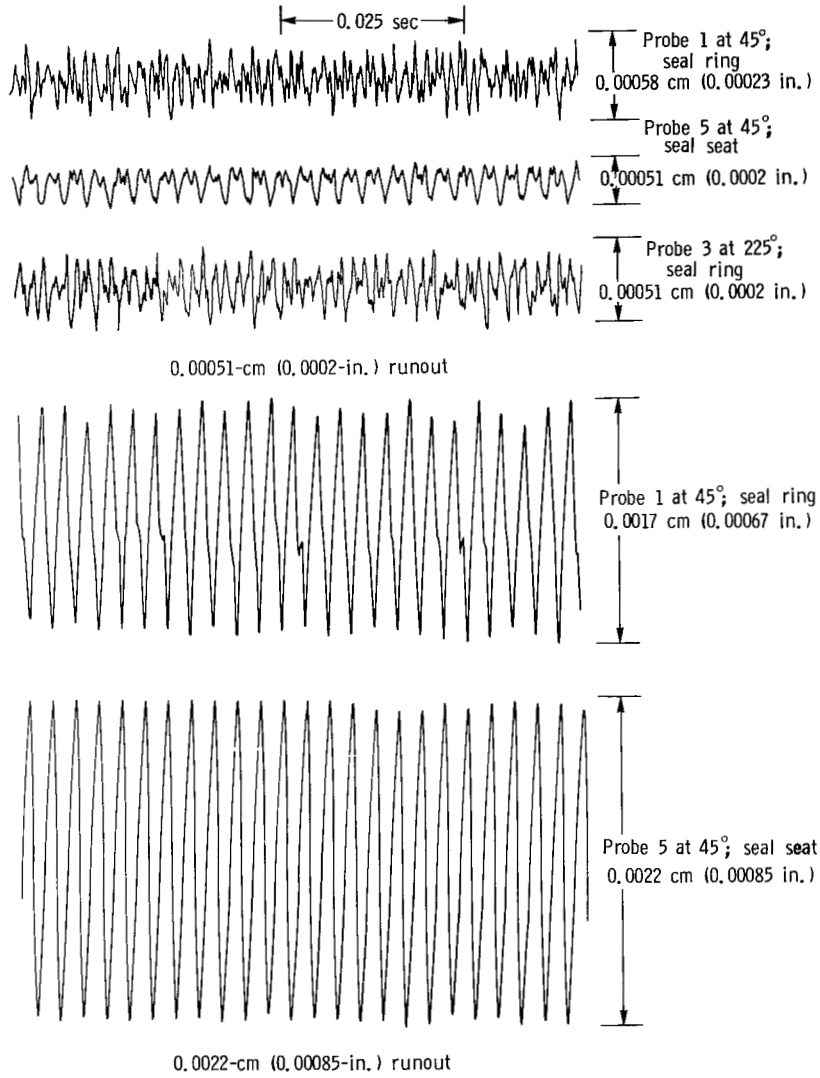

Figure 9. - Oscillograph traces showing effect of seal seat face runout on seal ring movement (relative to seal seat face) under light spring load condition. Recess-pad length to land-length ratio, 2:1; recess-pad depth, 0.0013 centimeter (0.0005 in.); sliding velocity, 61 meters per second (200 ft/sec); ambient pressure, 10 newtons per square centimeter (14.7 lb/in.^{2}); room temperature, 300 K (80 F); spring load, 1.13 kilograms (2.50 lb); two seal seat face runouts.

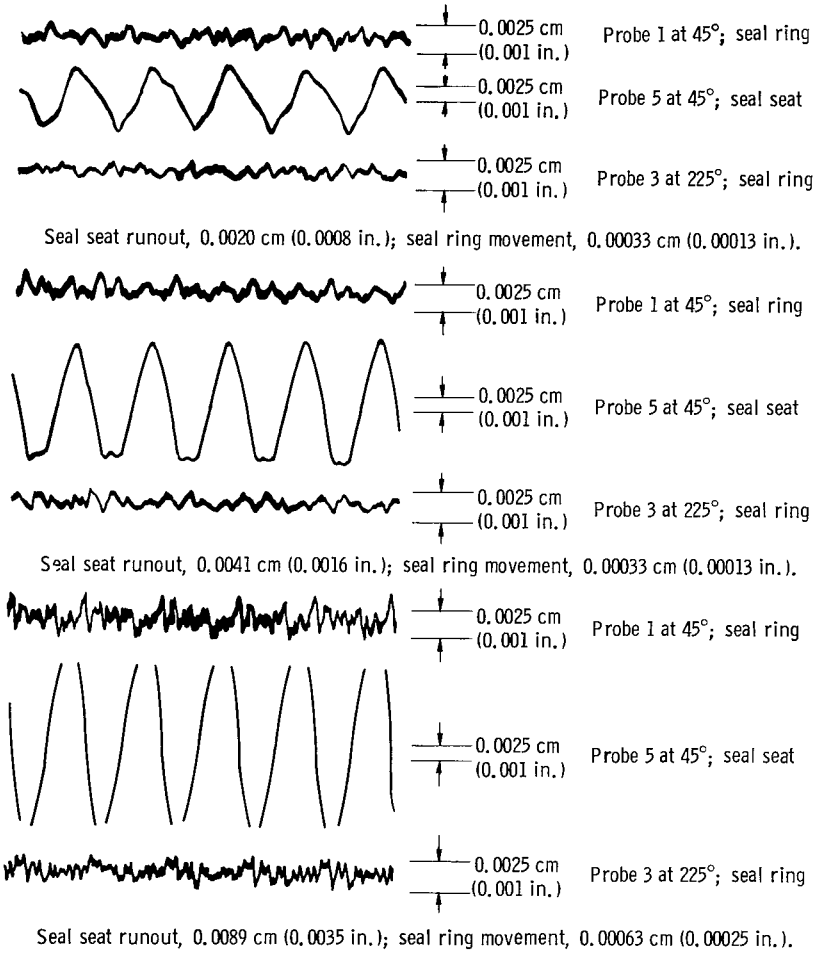

Figure 10. - Oscilloscope traces showing effect (relative to seal seat face) of seal seat face runout (due to shaft instability) on seal ring movement at maximum spring load. Recess-pad-length to land-length ratio, 2:1; recess-pad depth, 0.0013 centimeter (0.0005 in.); sliding velocity, 61 meters per second (200 ft/sec); ambient pressure, 10 newtons per square centimeter (14.7 lb/in.^{2}); room temperature, 300 K (80° F); spring load, 12.5 kilograms (27.5 lb).

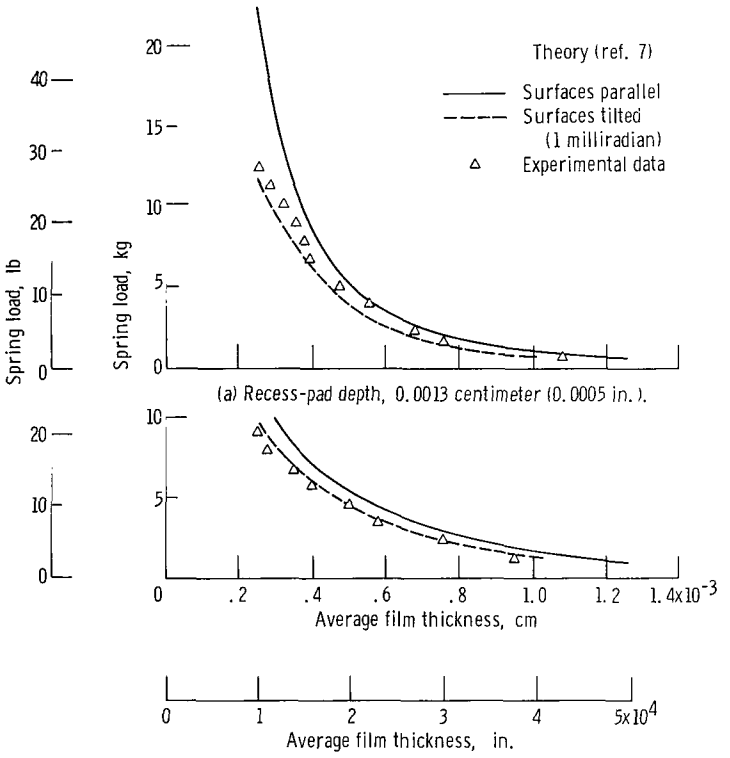

(a) Recess-pad depth, 0.0013 centimeter (0.0005 in.).

(b) Recess-pad depth, 0.0025 centimeter (0.001 in.).

Figure 11. - Load capacity as function of mean film thickness for Rayleigh step-pad geometry. Recess-pad-length to land-length ratio, 2:1; 15 pads; sliding velocity, 61 meters per second (200 ft/sec); ambient pressure, 14.7 newtons per square meter (10 lb/in.^{2}); temperature, 300 K (80^0 F).

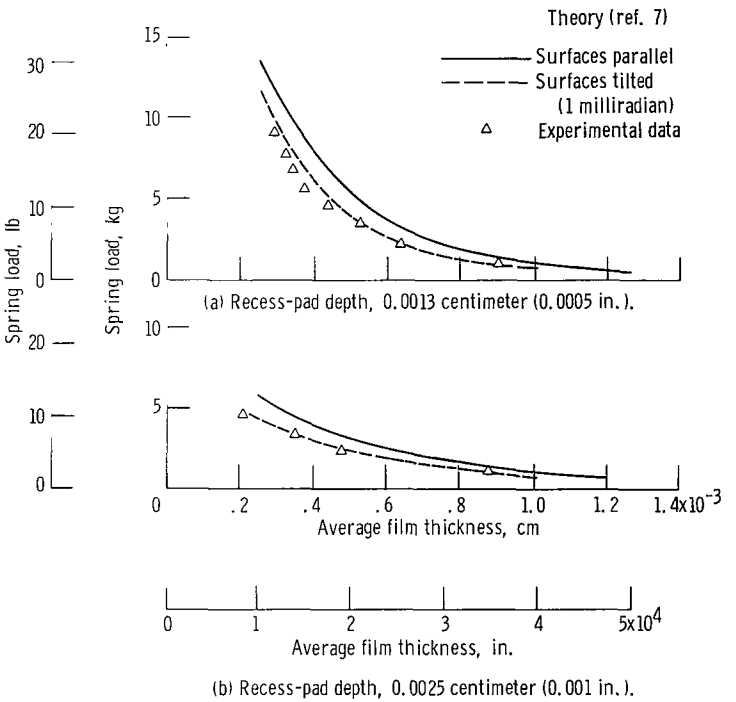

(a) Recess-pad depth, 0.0013 centimeter (0.0005 in.).

(b) Recess-pad depth, 0.0025 centimeter (0.001 in.).

Figure 12. - Load capacity as function of mean film thickness for Rayleigh step-pad geometry. Recess-pad-length to land-length ratio, 1.1; 15 pads; sliding velocity, 61 meters per second (200 ft/sec); ambient pressure, 14.7 newtons per square meter (10 lb/in.^{2}); temperature, 300 K (80^0 F).

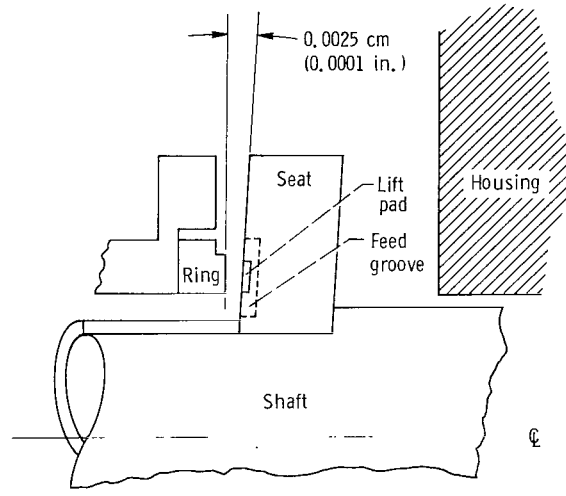

Figure 13. - Seal with exaggerated face deformation (diverging angular tilt).

NASA-Langley, 1971 —— 15 E-6186

"The aeronautical and space activities of the United States shall be conducted so as to contribute . . . to the expansion of human knowledge of phenomena in the atmosphere and space. The Administration shall provide for the widest practicable and appropriate dissemination of information concerning its activities and the results thereof."

—NATIONAL AERONAUTICS AND SPACE ACT OF 1958

NASA SCIENTIFIC AND TECHNICAL PUBLICATIONS

TECHNICAL REPORTS: Scientific and technical information considered important, complete, and a lasting contribution to existing knowledge.

TECHNICAL NOTES: Information less broad in scope but nevertheless of importance as a contribution to existing knowledge.

TECHNICAL MEMORANDUMS: Information receiving limited distribution because of preliminary data, security classification, or other reasons.

CONTRACTOR REPORTS: Scientific and technical information generated under a NASA contract or grant and considered an important contribution to existing knowledge.

TECHNICAL TRANSLATIONS: Information published in a foreign language considered to merit NASA distribution in English.

SPECIAL PUBLICATIONS: Information derived from or of value to NASA activities. Publications include conference proceedings, monographs, data compilations, handbooks, sourcebooks, and special bibliographies.

TECHNOLOGY UTILIZATION PUBLICATIONS: Information on technology used by NASA that may be of particular interest in commercial and other non-aerospace applications. Publications include Tech Briefs, Technology Utilization Reports and Technology Surveys.

Details on the availability of these publications may be obtained from:

SCIENTIFIC AND TECHNICAL INFORMATION OFFICE

NATIONAL AERONAUTICS AND SPACE ADMINISTRATION

Washington, D.C. 20546